

Service-Life Prediction of Reinforced Concrete Structures under Corrosive Environment

Takumi Shimomura

Department of Civil and Environmental Engineering, Nagaoka University of Technology
1603-1 Kamitomiokamachi, Nagaoka, Niigata 940-2188, JAPAN

A comprehensive framework for numerical simulation of time-dependent performance change of reinforced concrete (RC) structures subjected to chloride attack is presented in this paper. The system is composed of simplified computational models for transport of moisture and chloride ions in concrete pore structure and crack, corrosion of reinforcement in concrete and mechanical behavior of RC member with reinforcement corrosion. Service-life of RC structures under various conditions is calculated.

Keywords: reinforced concrete, corrosion, chloride, RC structure, life prediction

1. Introduction

In general, performance of a concrete structure under service is gradually deteriorated by loading and environmental attack under service. In order to ensure rational service-life design of concrete structures to be built and to ensure rational ageing management of existing concrete structures, therefore, it would be useful to develop an engineering prediction method for performance of concrete structures as a function of service time. Fig. 1 schematically shows the estimated service-life of concrete structures considering upgrading, i.e., repair or rehabilitation, techniques. If we can calculate time-dependent change of structural performance of concrete structures under arbitrary conditions, we can know residual service-life of the structures as the length of time until the calculated value of structural performance meets the minimum acceptable performance.

If no special maintenance operations are taken during the service-life of a structure, its residual service-life is assumed (a) in Fig. 1. On the other hand, if we execute some upgrading operation at the time t_1 , the residual service-life of the structure can be extended as (b) and (c). To evaluate the length of the residual service-life of the structure accurately, we should be able to calculate performance of the structure as a function of service time taking possible upgrading techniques into consideration.

Though it is too simplified discussion compared with

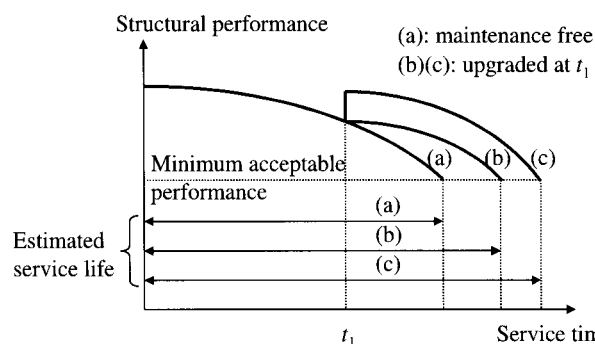


Fig. 1. Schematic illustration of estimated service-life of concrete structures

real cases, this is a basic concept for ideal service-life management of concrete structures. Thus, the author has been working to develop and improve a numerical service-life simulation system for concrete structures, in which upgrading techniques can be considered. In this paper, the outline of this methodology is reviewed with recent research progress.

2. Outline of the methodology

The outline of the computational system considered in this study is shown in Fig. 2. Degradation process of concrete structures is calculated step by step with respect to service time by coupling mathematical models for microscopic phenomena in concrete. Since corrosion of reinforcing steel bars embedded in concrete is one of the typical and the serious degradation phenomena of general concrete structures, corrosion problem is focused on here.

[†] Corresponding author: takumi@nagaokaut.ac.jp

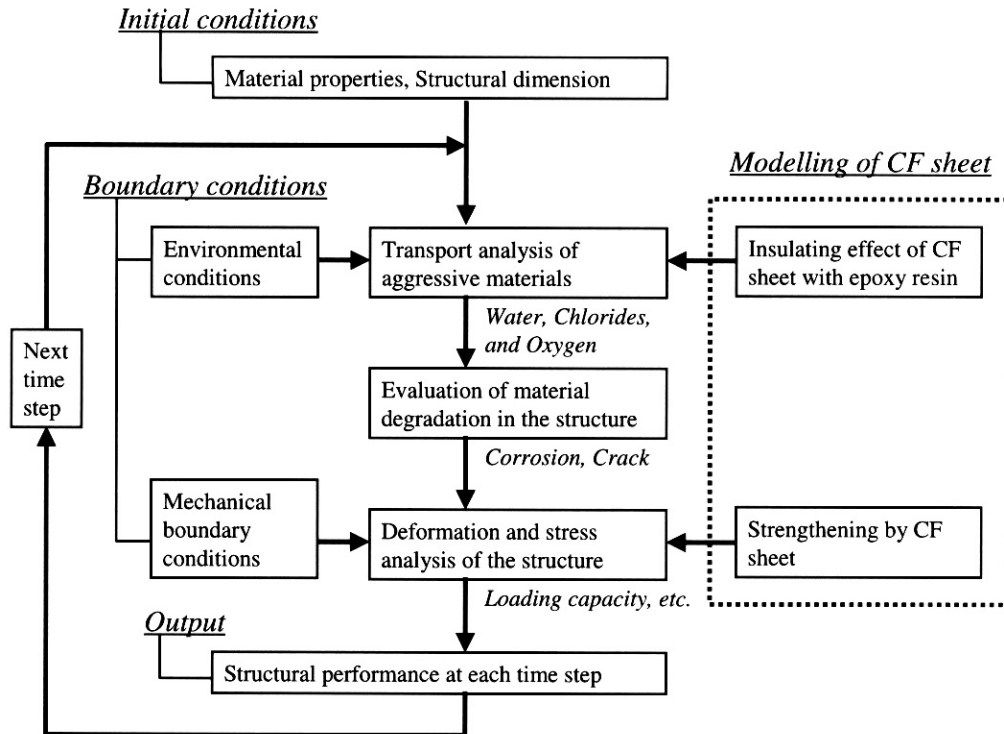


Fig. 2. Outline of the computational system

Hence, we calculate chloride ingress into concrete, corrosion of reinforcement in concrete and structural performance of members with corroded reinforcements at each time step. As results, structural performance is evaluated as a function of time.

One of the advantages of this method is that we can naturally consider the influences of various factors, such as material selection, structural dimension, environmental conditions and upgrading techniques, on the service-life of structures in terms of the formulated computational models based on the mechanisms of the corresponding phenomena. In this paper, upgrading method using continuous fiber (CF) sheet is considered: carbon or aramid CF sheet is bonded on the surface of existing concrete structures with epoxy resin.

3. Formulations

3.1 Pore structure of concrete

Aggressive materials, which are water, chloride ions and oxygen, are transported through common concrete porous media. Therefore, in order to rationally simulate transport phenomena of these aggressive materials in concrete, pore structure of concrete is mathematically expressed using the following statistical pore size distribution function.¹⁻²⁾

$$V(r) = V_o \{1 - \exp(-Br^c)\} \quad (1)$$

where r = pore radius; $V(r)$ = pore volume fraction whose radius is less than r ; V_o = total porosity; and B and C = parameters which determine characteristics of pore size distribution. The values of V_o , B and C can be determined from measured pore size distribution of concrete or can be empirically estimated from concrete mix proportion and curing conditions.

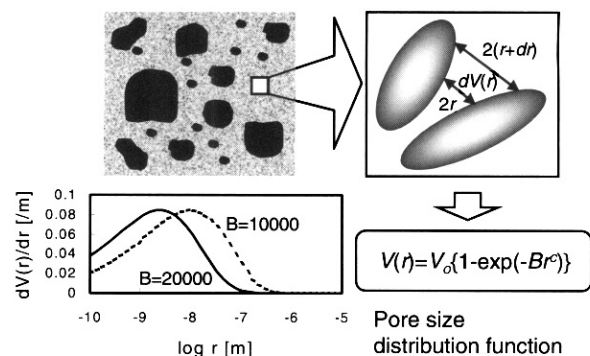


Fig. 3. Modeling of pore structure of concrete

3.2 Material transport in concrete

Water in concrete micro pore is treated as two-phase material: vapor and liquid water.

$$\frac{\partial w}{\partial t} = -div(J_v + J_l) \quad (2)$$

where w = mass concentration of water per unit concrete volume; t = time; and J_v and J_l = mass flux of vapor and liquid water respectively, both of which are calculated by the author's computational model based on thermodynamic behavior of water in porous media.

$$J_v = \int_{r_s}^{\infty} \left\{ \frac{dV(r)}{dr} (-K_v D_{vo} grad \rho_v) \right\} dr \quad (3)$$

$$J_l = \int_0^{r_s} \left[\rho_l \frac{dV(r)}{dr} \left\{ -K_l \frac{r^2}{8\mu} grad \left(-\frac{2\gamma}{r_s} \right) \right\} \right] dr \quad (4)$$

where r_s = radius of the pore in which the interface between vapor and liquid water is developed; ρ_v and ρ_l = density of vapor and liquid water respectively; D_{vo} = diffusivity of vapor; μ = viscosity of liquid water; γ = surface tension of liquid water; and K_v and K_l = non-dimensional material factors representing tortuosity of pore structure. The original moisture transport model can be applied only to non-saturated concrete exposed to humid atmosphere. However, in order to evaluate adequately moisture transport in concrete structures under real corrosive environment, it is necessary to consider capillary suction of liquid water from the concrete surface associated with splashed seawater and rainfall. It is assumed that capillary suction through larger concrete pores occurs during the concrete surface directly contacts with liquid water. Thus, in wetting process:

$$J_l = \int_{t_{cap}}^{\infty} \left(\rho_l \frac{dV(r)}{dr} \sqrt{K_l \frac{r\gamma}{8\mu t_{cap}}} \right) dr \quad (5)$$

where r_{cap} = radius of the narrowest pore in which capillary suction occurs; and t_{cap} = time from the beginning of wetting process. In order to predict chloride ingress into concrete under real corrosive environment, it should be significant to account capillary suction in computation, because chloride ions are partly carried by liquid water.

Transport of chloride ions in concrete pores is calculated with considering molecular diffusion of free chloride ions within liquid water phase, bulk mass flux of free chloride ions carried by liquid water, and transition between free

and fixed chloride with cement hydrate in concrete:

$$\frac{\partial C_{clt}}{\partial t} = -div \left(J_{Cl_{dif}} + C_{Clf} \frac{J_l}{\rho_l} \right) \quad (6)$$

where C_{clt} = total mass concentration of chloride per unit concrete volume; $J_{Cl_{dif}}$ = mass flux of chloride by molecular diffusion; and C_{Clf} = mass concentration of free chloride. The last term in Equation 6 expresses mass flux of chloride ions carried by liquid water that can be obtained from the moisture transport analysis. This is why coupling analysis between moisture and chloride ions is essential in predicting transport of chloride ions in concrete. The mass flux of chloride ions by molecular diffusion is calculated as:

$$J_{Cl_{dif}} = -K_{Cl} D_{Cl} grad C_{Clf} \quad (7)$$

where K_{Cl} = non-dimensional material factor that is assumed the same value as K_v in this study; D_{Cl} = diffusivity of chloride ion in liquid water. Transition between free and fixed chloride is calculated based on their equilibrium:

$$C_{Clf} = (1 - \alpha(C_{clt})) \cdot C_{clt} \quad (8)$$

where $\alpha(C_{clt})$ = fixing rate of chloride ions with cement hydrate in hardened concrete that was empirically formulated as a function of C_{clt} and the type of cement.³⁾

To calculate corrosion rate of steel embedded in concrete, the concentration of oxygen around the steel bar at each time step is needed. Transport of oxygen in concrete is calculated by the microstructure-based diffusion model, in which diffusion in gas and liquid phase and Henry's law of solution are taken into account. Transport of oxygen in concrete cover is calculated based on the assumption that mass concentration of oxygen is assumed zero at the surface of steel, because oxygen is consumed by corrosion reaction of steel.

3.3 Material permeability of layer of CF sheet and epoxy resin

An electrical permeability test was employed to quantify the material permeability of the layer of continuous fiber (CF) sheet and epoxy resin. Cylindrical concrete specimens shown in Fig. 4 were used in the test. Twelve specimens, whose experimental parameters are water-cement ratio of concrete, thickness of concrete cover and wrapping of CF sheet on the surface, were tested. Setup for the permeability test is shown in Fig. 5. Constant electric voltage of 30V was applied to the specimen in NaCl

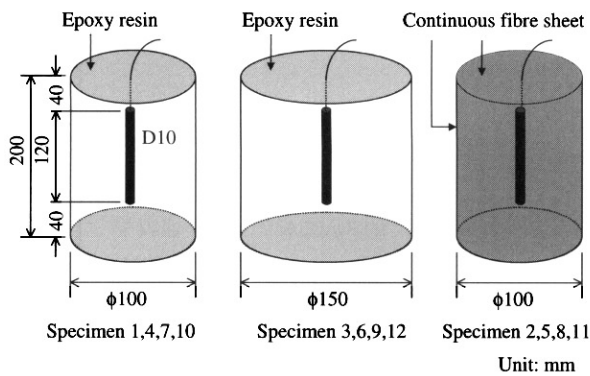


Fig. 4. Cylindrical specimen for permeability test

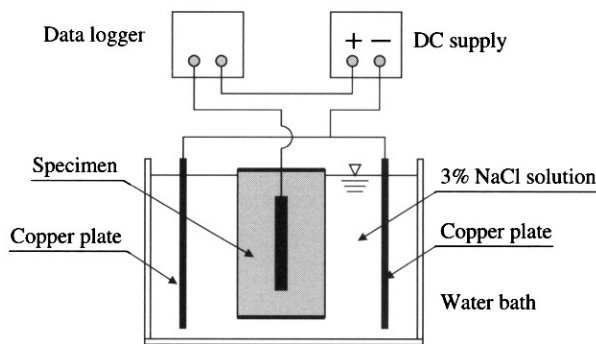


Fig. 5. Setup for chloride permeability test

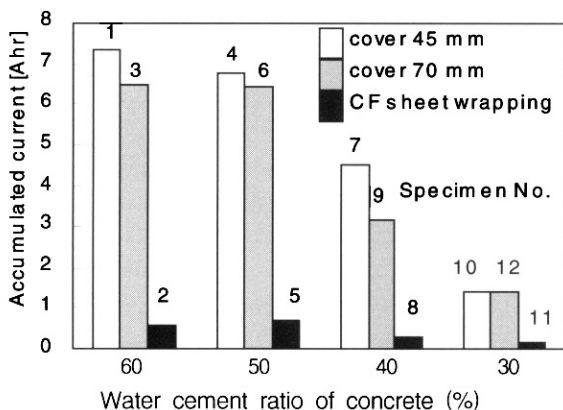


Fig. 6. Accumulated electric current of the specimens until 90 hours

solution. Time-dependent direct current penetrating the concrete was measured. Accumulated electric current until 90 hours is taken as an index for permeability of specimen as shown in Fig. 6. Based on these test results, diffusion coefficient of the layer of CF sheet and epoxy resin was quantified as $3 \times 10^{-14} \text{ m}^2/\text{s}$, which is approximately two orders as small as that of ordinary concrete.⁴⁾

3.4 Corrosion of reinforcement in concrete

Corrosion rate of the reinforcing steel bar in concrete

at each time step is calculated by the simplified model based on the fundamental theory of electrode kinetics of corrosion. Depassivation of steel due to chloride, activation polarization, and concentration polarization are considered. Accordingly, corrosion rate depends on chloride concentration at the bar portion and mass flux of oxygen in concrete cover, both of which are obtained from transport analysis. In reality, corrosive state of steel bars in concrete varies with sections because of flexural cracks, some initial defects of concrete cover, and difference of boundary conditions. However, uniform corrosion along the bar shown in Fig. 7 is assumed in this study to simplify the computation. Based on this modeling, loss of effective cross sectional area and corrosive expansion of the bar are calculated.

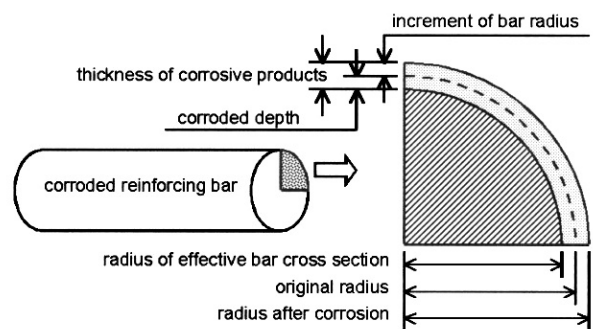


Fig. 7. Model for corroded reinforcing steel bar

3.5 Corrosion crack in concrete

The occurrence of corrosion crack in concrete cover due to corrosive expansion of the reinforcing bar is predicted by the elastic stress analysis of concrete around the bar. After cracking, crack width is calculated by the simplified two-dimensional rigid rotational model shown in Fig. 8.⁵⁻⁶⁾

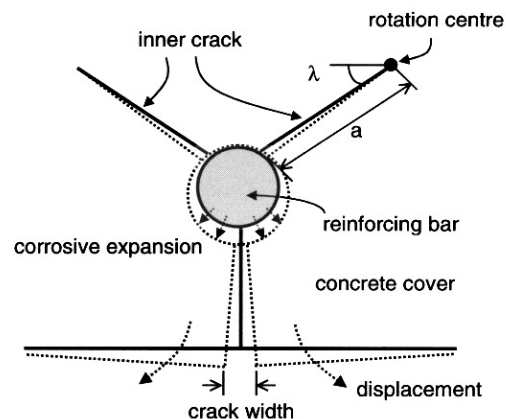


Fig. 8. Model for corrosion crack

3.6 Structural behavior of RC member with reinforcement corrosion

Following mechanisms are considered in the computation of structural behavior of RC member with corroded reinforcing bars:

- reduction of effective cross sectional area of bar,
- reduction of tensile stress carried by concrete around the bar by bonding mechanisms,
- slip between bar and concrete.

In the proposed simulation system, all the above items are quantitatively considered in terms of corresponding mechanical models. Among those, bar cross sectional area is the most important from the viewpoint of ultimate load carrying capacity of RC members. The residual effective cross sectional area of corroded bar can be calculated from the amount of corrosion as shown in Fig. 7. The second and the third items result from deterioration of bonding between bar and concrete due to corrosion, which affect crack pattern or deformability of members more than load carrying capacity.

The tensile stress carried by concrete around the bar by bonding mechanisms is calculated by the tension-stiffening model.⁷⁾

$$\sigma_c = f_t \left(\frac{\epsilon_u}{\epsilon} \right)^\alpha \tag{9}$$

where σ_c = average stress of concrete; f_t = tensile strength of concrete; ϵ_u = cracking strain of concrete; ϵ = average strain; and α = the parameter representing bond characteristics. The original tension-stiffening model was proposed for non-corroded bar, in which the value of α was 0.4. The authors assume that, for corroded bar, α depends on degree of corrosion of the bar as shown in Fig. 9. Tension-stiffness of RC member with reinforcement corrosion is also experimentally measured by laboratory test.⁸⁾

The slip between bar and concrete is formulated as:

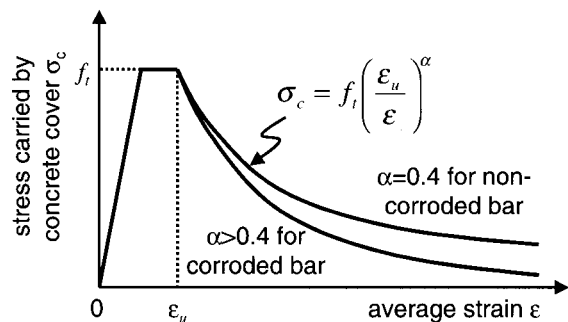


Fig. 9. Tension-stiffening model for concrete around corroded reinforcing bar

$$\epsilon_s(x) = K_s \left(\frac{1}{l_c} \int_0^{l_c} \epsilon_{cs}(\xi) d\xi - \epsilon_{cs}(x) \right) + \epsilon_{cs}(x) \tag{10}$$

where $\epsilon_s(x)$ = strain of bar; K_s = the parameter representing degree of slip; l_c = length of the corroded region; and $\epsilon_{cs}(x)$ = strain of concrete at the bar portion. The parameter K_s is set zero for perfect bond state as ordinary RC member and 1 for unbond state where strain of bar uniformly distributes. In case of corroded bar, K_s is determined as a function of the degree of corrosion.

3.7 Strengthening by CF sheet

Formula for external bonding with CF sheet was derived with interfacial fracture energy between CF sheet and concrete, G_f as follows.⁹⁾

$$\sigma_f \leq \sqrt{\frac{2G_f E_f}{n_f \cdot t_f}} \tag{11}$$

where σ_f = CF sheet stress at flexural crack caused by maximum moment; n_f = number of sheet layers; and t_f = thickness of sheet. Interfacial fracture energy G_f is obtained by pull-out test of CF sheet bonded to concrete, otherwise $G_f = 0.5$ (N/mm) may be assumed. If Equation 11 is satisfied, no delamination of CF sheet would occur. Then ultimate flexural capacity of the member retrofitted with CF sheet can be calculated by the conventional bending theory on the basis of the following assumptions as shown in Fig. 10:

- CF sheet is perfectly bonded on the surface of concrete.
- strain of CF sheet is proportional to the distance from the neutral axis.

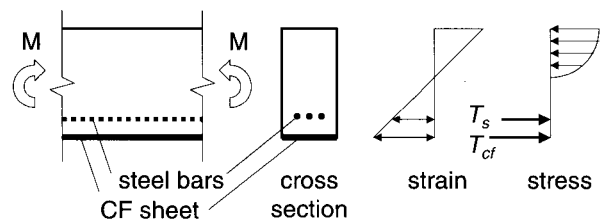


Fig. 10. Flexural stress in RC member with CF sheet

4. Numerical simulations

4.1 Analytical series

To demonstrate the applicability of the proposed methodology, service-life simulation of concrete structure was carried out; flexural capacity of RC beam under various conditions were calculated as a function of service time. RC beam analyzed in the standard case is shown

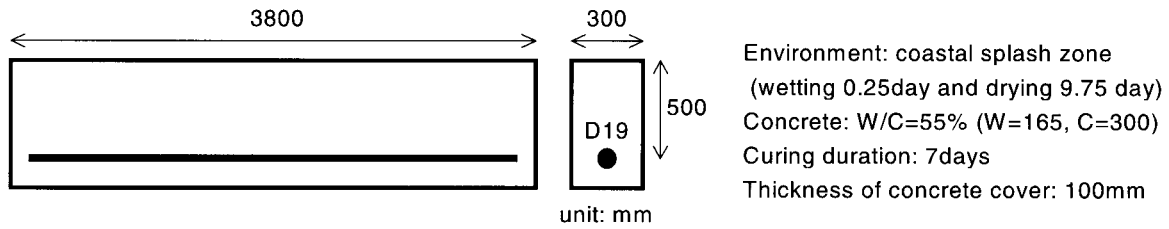


Fig. 11. Analyzed RC beam (standard case)

in Fig. 11. The environmental condition in the standard case is exposure to seawater for 0.25 day every 10 days, which simulates a splash zone near the coast. Material parameters of concrete, which are strength, pore size distribution and transport coefficients, are estimated from the mix proportion and curing duration of concrete.

Three series, which include ten cases in total, are analyzed:

1. Sensitivity analysis of environmental condition in which the structure is exposed during its service life.
 2. Sensitivity analysis of initial condition of the structure, which are mix-proportion and curing duration of concrete and thickness of concrete cover.
 3. Sensitivity analysis of upgrading method applied to structures under service, which are desalination (removing chlorides from concrete) and retrofit-ting of CF sheet.
- When desalination is applied, chloride in concrete cover is assumed once completely removed. CF sheet is treated as elastic material.

4.2 Results and discussion

Fig. 12 shows analytical results of the series 1, indicating the relationship between flexural capacities of the beam normalized by initial value and service time. Steel bars in concrete under cyclic wetting-drying environment, which simulate splash zone or shoreline, are corroded faster than that under constant environment as in the seawater or in the air.

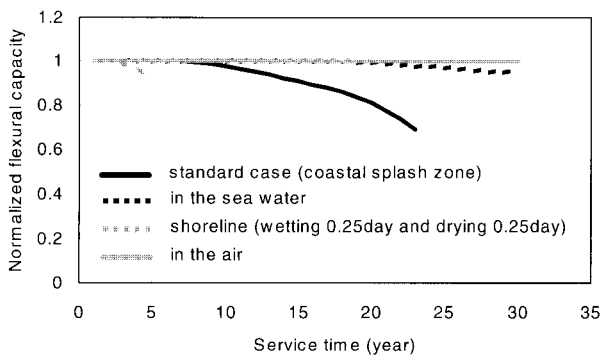


Fig. 12. Results of the series 1: sensitivity analysis of environmental condition

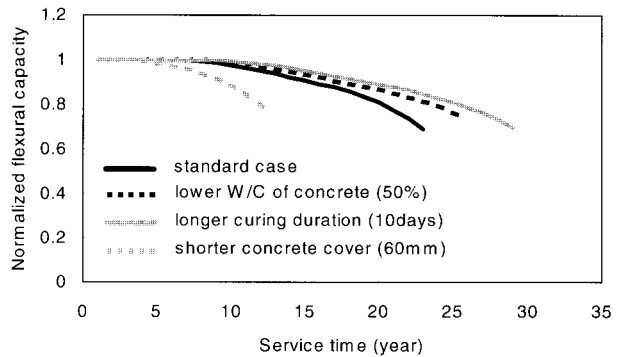


Fig. 13. Results of the series 2: sensitivity analysis of initial condition

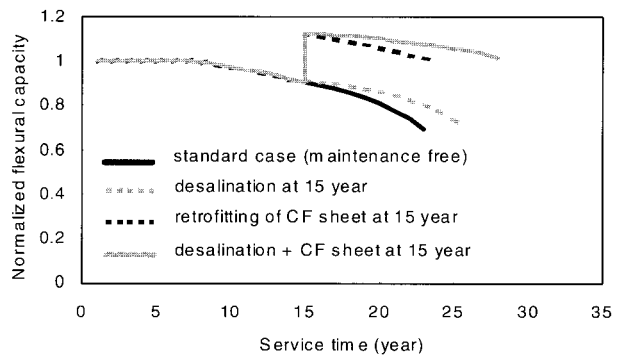


Fig. 14. Results of the series 3: sensitivity analysis of upgrading method

Analytical results of the series 2 are shown in Fig. 13. In cases that concrete with lower water-cement ratio is used or longer curing period is provided, degradation of flexural capacity is retarded, which means service-life of the structure is extended. On the contrary, in case that shorter cover depth is provided, the flexural capacity of the beam is degraded earlier.

Analytical results of the series 3 are shown in Fig. 14. In case that desalination is applied at 15 years, corrosion of steel is once stopped, but after several years since then, corrosion starts again because chloride gradually comes into concrete again. In case that CF sheet is retrofitted, flexural capacity of the beam is strengthened and therefore

its service-life is extended. However, without desalination, corrosion of the bar does not stop even after retrofitting of CF sheet due to remaining chloride in concrete, though corrosion rate is reduced because of low permeability of CF sheet. If both desalination and CF sheet are applied, corrosion of bar is effectively stopped, because CF sheet prevents new chloride ingress.

5. Conclusions

A framework of service-life prediction of concrete structures by numerical simulation was presented. Performance of concrete structures with assumed material selections and structural dimension under given environmental condition can be evaluated as a function of service time, while effectiveness of up-grading techniques, such as retrofitting of CF sheet, on service-life extension are considered. The computational results by the proposed method showed that the program could reasonably account the influences of environmental conditions, initial conditions and upgrading techniques on the service life of the concrete structures. Consequently, the proposed simulation method will be helpful for both service-life design of new structures and aging management of existing structures.

References

1. T. Shimomura and K. Maekawa, *Proceedings of the 5th International RILEM Symposium on Creep and Shrinkage of Concrete*, Z. P. Bazant and I. Carol (Eds.), p.133, London, E & FN Spon (1993).
2. T. Shimomura and K. Maekawa, *Magazine of Concrete Research*, **49**(181), 303 (1997).
3. T. Maruya, *Concrete Library of JSCE*, **20**, 57 (1992).
4. H. Kasahara, T. Shimomura, and Y. Chenna, *Proceedings of the Japan Concrete Institute*, **25**(1), 311 (2003) in Japanese.
5. T. Shimomura, *Proceedings of the International Conference on Life Prediction and Aging Management of Concrete Structures*, p.128, Bratislava, EXPERTCENTRUM, (1999).
6. M. Okazaki, T. Shimomura, and H. Matsuo, *Proceedings of the Japan Concrete Institute*, **25**(1), 857 (2003) in Japanese.
7. H. Okamura, *Proceedings of the Seminar ASCE*, (1985).
8. T. Shimomura, M. Okazaki, H. Matsuo, and K. Maruyama, *Proceedings of the 4th International Conference on Concrete under Severe Conditions: Environment & Loading*, Seoul (2004). to be presented.
9. Japan Society of Civil Engineers (JSCE), *Recommendations for Upgrading of Concrete Structures with Use of Continuous Fiber Sheets*, Tokyo: JSCE, 2001.